

Signatures of entanglement and quantum phase transitions in parallel quantum dots

Arturo Wong,¹ W. Brian Lane,² Luis G. G. V. Dias da Silva,³ Kevin Ingersent,⁴ Nancy Sandler,¹ and Sergio E. Ulloa¹

¹*Department of Physics and Astronomy, Nanoscale and Quantum Phenomena Institute, Ohio University, Athens, Ohio 45701, USA*

²*Department of Physics, Jacksonville University, 2800 University Boulevard North, Jacksonville, Florida 32211, USA*

³*Instituto de Física, Universidade de São Paulo, C.P. 66318, 05315-970 São Paulo, SP, Brazil*

⁴*Department of Physics, University of Florida, P.O. Box 118440, Gainesville, Florida 32611, USA*
(Dated: February 17, 2019)

We study a strongly interacting “quantum dot 1” and a weakly interacting “dot 2” connected in parallel to metallic leads. Gate voltages can drive the system between Kondo-quenched and free-moment phases separated by Kosterlitz-Thouless quantum phase transitions. As interactions in dot 2 become stronger relative to the dot-lead coupling, the free moment evolves from an isolated spin- $\frac{1}{2}$ in dot 1 to a many-body doublet arising from an underscreened Kondo effect. These limits, which feature very different entanglements between dot and lead electrons, can be distinguished by conductance measurements at finite temperatures.

Semiconductor quantum dots afford a level of experimental control that has made them the premier setting [1] in which to investigate the Kondo effect: the many-body screening of a local moment by delocalized electrons. In recent years, interest has turned from Kondo physics in single dots to similar phenomena in more complex structures such as double-dot devices [2, 3], where quantum phase transitions (QPTs) have been predicted [4–8] and possibly observed [3].

Double quantum dots (or two levels within a single dot) connected in parallel to the same leads have been studied theoretically in two disparate limits: (I) Systems in which each dot has strong Coulomb interactions and can acquire a magnetic moment [5, 8] exhibit a Fermi-liquid phase with a singlet ground state and a “singular Fermi liquid” phase having a residual spin- $\frac{1}{2}$ arising from an underscreened spin-1 Kondo effect [9]. These phases are separated by lines of Kosterlitz-Thouless QPTs broken by first-order QPTs at high-symmetry points [8]. (II) An interacting dot 1 and a noninteracting (nonmagnetic) dot 2 [6] can realize the pseudogap Kondo effect [10, 11], with a Kondo-screened phase and a non-Kondo local-moment phase separated by first-order QPTs having clear signatures in finite-temperature transport [7].

In this Letter we explore the connection between limits I and II above by considering the effect of increasing the dot-2 Coulomb interaction U_2 from zero. A free-moment (FM) phase with an unquenched spin- $\frac{1}{2}$ occupies a region of parameter space that grows with U_2 and is separated from a surrounding strong-coupling (SC) phase by Kosterlitz-Thouless QPTs. For $U_2 \lesssim \Gamma_2$, the level width of dot 2 due to its coupling to the leads, the properties retain signatures of the $U_2 = 0$ pseudogap Kondo physics, while for $U_2 \gg \Gamma_2$, there is a smooth crossover to limit I. These two regimes, which both exhibit singular Fermi liquid behavior but have very different dot-lead entanglements, can be distinguished through conductance measurements at experimentally accessible temperatures.

In experiments, it is impractical to adjust U_2 by orders of magnitude, but the crossover from $U_2 \ll \Gamma_2$ to $U_2 \gg \Gamma_2$ can be accessed by tuning Γ_2 via gate voltages. The setup therefore has great potential for controlled investigation of QPTs and of entanglement in singular Fermi liquids, which lie on the borderline between regular Fermi liquids and non-Fermi liquids [12].

We consider a generalized Anderson Hamiltonian $H = H_{\text{dots}} + H_{\text{leads}} + H_{\text{mix}}$, where $H_{\text{dots}} = \sum_i (\varepsilon_i n_i + U_i n_{i\uparrow} n_{i\downarrow})$ with $n_i = \sum_{\sigma} n_{i\sigma} = \sum_{\sigma} d_{i\sigma}^{\dagger} d_{i\sigma}$ describes the highest partially-occupied level in dots $i = 1$ and 2 , $H_{\text{leads}} = \sum_{j\mathbf{k}\sigma} \epsilon_{j\mathbf{k}} c_{j\mathbf{k}\sigma}^{\dagger} c_{j\mathbf{k}\sigma}$ models left and right ($j = L, R$) leads, and $H_{\text{mix}} = \sum_{ij\mathbf{k}\sigma} V_{ij} (d_{i\sigma}^{\dagger} c_{j\mathbf{k}\sigma} + \text{H.c.})$ accounts for electron tunneling between dots and leads. For simplicity, we take real, local dot-lead couplings $V_{iL} = V_{iR} \equiv V_i/\sqrt{2}$, in which case the dots interact only with one effective band formed by an even-parity combination of L and R states. We assume a constant density of states $\rho = 1/(2D)$ with half bandwidth D , so that the dot-lead tunneling is measured via the hybridization widths $\Gamma_i = \pi \rho V_i^2$. At low bias, electron transmission described by a Landauer-like formula [13] gives a linear conductance

$$g = \frac{2e^2}{h} \int d\omega \left(\frac{-\partial f}{\partial \omega} \right) \pi \sum_{i,j} \sqrt{\Gamma_i \Gamma_j} A_{ij}(\omega, T), \quad (1)$$

where $f(\omega, T)$ is the Fermi function and $A_{ij}(\omega) = -\pi^{-1} \text{Im} G_{ij}(\omega)$, with $G_{ij}(t) = -i\theta(t) \langle \{d_{i,\sigma}(t), d_{j,\sigma}^{\dagger}(0)\} \rangle$ being a retarded Green’s function.

We have studied this model using the numerical renormalization-group [14] with discretization parameter $\Lambda = 2.5$, retaining at least 1000 states after each iteration. This Letter focuses on the representative case of a strongly interacting dot 1 described by $U_1 = 10\Gamma_1 = 0.5D$ and a dot-2 hybridization width $\Gamma_2 = 0.02D$. We show the variation of physical properties with temperature T and the dot energies ε_i (which should be experimentally tunable via plunger gate voltages) for different

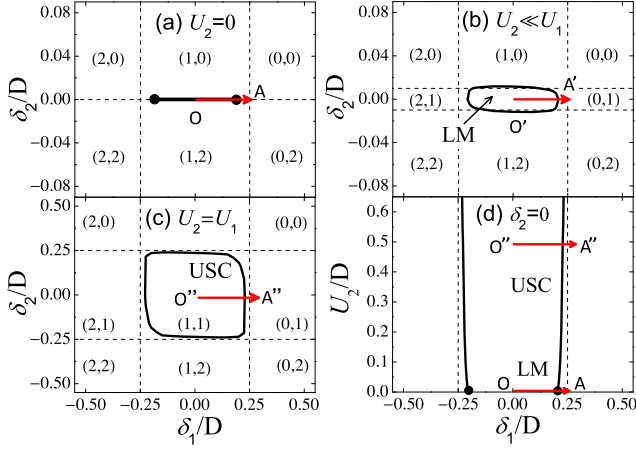


FIG. 1: (Color online). Ground states of the isolated double QDs [dashed lines and dot occupancies ($\langle n_1 \rangle, \langle n_2 \rangle$)] and phases of the full system for $\Gamma_1 = 0.05D$, $\Gamma_2 = 0.02D$ (solid lines) vs level energies $\delta_i = \varepsilon_i + \frac{1}{2}U_i$ measured from p-h symmetry for (a) $U_2 = 0$, (b) $U_2 = 0.02D \ll U_1$ and (c) $U_2 = U_1$. (d) Phase diagram of the full system on the δ_1 - U_2 plane at $\delta_2 = 0$, showing local-moment (LM) and underscreened spin-1 Kondo (USC) regimes within the free-moment phase.

values of U_2 [15]. We reiterate that in real devices, U_2 will likely be fixed and Γ_2 instead will be varied.

It is instructive first to consider the dots isolated from the leads, *i.e.*, $\Gamma_1 = \Gamma_2 = 0$. Figures 1(a)–1(c) show $T = 0$ occupancies ($\langle n_1 \rangle, \langle n_2 \rangle$) vs the level energies $\delta_i = \varepsilon_i + \frac{1}{2}U_i$ measured from particle-hole (p-h) symmetry for $U_2 = 0, 0.02D (\ll U_1)$ and $0.5D (= U_1)$. The occupancies jump upon crossing any of the dashed lines $|\delta_i| = \frac{1}{2}U_i$. For $U_2 = 0$ [Fig. 1(a)], $\langle n_2 \rangle = 1$ only along the line $\delta_2 = 0$ and the δ_1 - δ_2 plane divides into six two-dimensional regions. For $U_2 > 0$ [Figs. 1(b,c)], there are instead nine regions, including three in which dot 2 is singly occupied and hence carries a moment.

When the dots are both connected to the metallic leads ($\Gamma_1, \Gamma_2 \neq 0$), we find that most of the δ_1 - δ_2 plane is occupied by an SC phase in which all dot degrees of freedom are quenched at $T = 0$. In this phase the first-order QPTs present for isolated dots (dashed lines in Fig. 1) are replaced by smooth crossovers between single-particle scattering of lead electrons (wherever both dots are empty or full, *i.e.*, $|\delta_i| \gg \frac{1}{2}U_i$ for $i = 1$ and 2) and many-body Kondo physics (where one of the dots is singly occupied, *i.e.*, $|\delta_i| \ll \frac{1}{2}U_i$). However, the region around the p-h symmetric point $\delta_1 = \delta_2 = 0$ forms a distinct FM phase in which a spin- $\frac{1}{2}$ degree of freedom survives to $T = 0$. With increasing U_2 , the FM phase grows (primarily along the δ_2 axis) as illustrated by the solid lines in Fig. 1.

The rest of the paper presents physical properties for $U_1 = 0.5D$, $\Gamma_1 = 0.05D$, and $\Gamma_2 = 0.02D$ along paths in parameter space crossing the phase boundaries, which we denote by $\varepsilon_1 = \varepsilon_1^\pm(U_2, \varepsilon_2)$. Our focus is on the regime $U_2 \lesssim \Gamma_2$ of a weakly correlated dot 2, but at the end we

consider cases where both dots have strong correlations.

We begin with the case $U_2 = 0$, studied previously using a mapping to an effective one-impurity model [6, 7], where the FM phase is restricted to $\varepsilon_2 = 0$, $\varepsilon_1^- < \varepsilon_1 < \varepsilon_1^+$ [$\varepsilon_1^\pm(0,0)$ being denoted by filled circles in Figs. 1(a,d)]. Figure 2(a) shows the temperature variation of χ_{imp} , the dot (“impurity”) contribution to the susceptibility, for several values of ε_1 along path OA in Figs. 1(a,d). In the FM phase (*e.g.*, $\varepsilon_1 = -\frac{1}{2}U_1$), a doublet ground state remains down to $T = 0$ with $T\chi_{\text{imp}} = \frac{1}{4}$. In the SC phase (*e.g.*, $\varepsilon_1 = -U_1/125$), the system instead has a singlet ground state and χ_{imp} (not just $T\chi_{\text{imp}}$) vanishes at $T \rightarrow 0$. For ε_1 close to ε_1^+ , singlet and doublet ground states are quasi-degenerate and $T\chi_{\text{imp}} \approx \frac{1}{6}$ within a window of temperatures above some T^* ; for $T \lesssim T^*$, there is a crossover to the low-temperature behavior of one or other phase. T^* goes to zero on approach to the phase boundary from either side, and at $\varepsilon_1 = \varepsilon_1^+$, $T\chi_{\text{imp}} = \frac{1}{6}$ down to $T = 0$. The inset to Fig. 2(b) shows that the Kondo temperature T_K —defined through the standard condition $T_K\chi_{\text{imp}}(T_K) = 0.0701$, and equal to T^* in the SC phase—vanishes linearly with $\Delta\varepsilon_1 = \varepsilon_1 - \varepsilon_1^+$, as expected at a first-order level-crossing QPT.

The first-order nature of the QPTs at $\varepsilon_1 = \varepsilon_1^\pm(0,0)$ can also be seen from the dot occupancies $\langle n_i \rangle$ at $T = 0$. On approach to the QPT from either phase, the occupancies [Fig. 2(b)] increasingly deviate from their values for isolated dots. Both occupancies undergo a jump at $\varepsilon_1 = \varepsilon_1^+$. The jump in $\langle n_1 \rangle$ equals the weight of a delta-function peak in the dot-1 spectral density that passes through the Fermi energy at the QPT [7]. In the limit where D greatly exceeds all other energy scales, $\langle n_1 + n_2 \rangle = n_{\text{imp}} \equiv \langle N \rangle - \langle N \rangle_0$, where $\langle N \rangle$ ($\langle N \rangle_0$) is the total number of electrons with (without) the dots [8]. One can find n_{imp} using the one-impurity pseudogap Anderson model onto which the full double-dot problem maps [6] for $U_2 = \varepsilon_2 = 0$. Since p-h asymmetry is irrel-

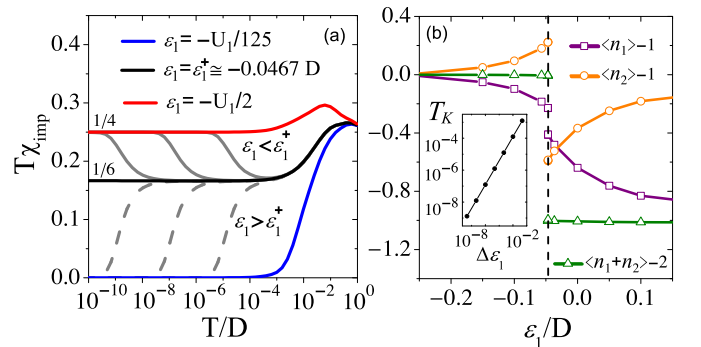


FIG. 2: (Color online). Non-interacting dot 2, $U_2 = \varepsilon_2 = 0$: (a) $T\chi_{\text{imp}}$ vs T for various values of ε_1 spanning the QPT at ε_1^+ . (b) $T = 0$ dot occupancies relative to half filling vs ε_1 , with a vertical dashed line at $\varepsilon_1 = \varepsilon_1^+$. Inset: Evolution of the Kondo scale showing a linear dependence on $\Delta\varepsilon_1 = \varepsilon_1 - \varepsilon_1^+$.

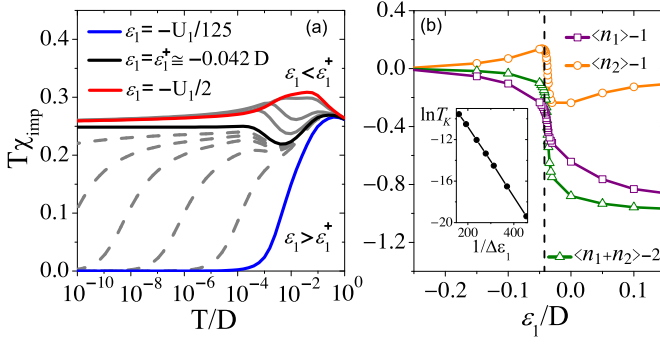


FIG. 3: (Color online). Interacting dot 2, $U_2 = -2\varepsilon_2 = \Gamma_2$: (a) $T\chi_{\text{imp}}$ vs T for various values of ε_1 spanning the QPT at ε_1^+ . (b) $T = 0$ dot occupancies relative to half filling vs ε_1 with a vertical dashed line at $\varepsilon_1 = \varepsilon_1^+$. Inset: Evolution of the Kondo scale T_K , showing $\ln T_K \propto 1/\Delta\varepsilon_1$ where $\Delta\varepsilon_1 = \varepsilon_1 - \varepsilon_1^+$.

evant (relevant) in the FM (SC) phase of the pseudogap model [11], $n_{\text{imp}}(T = 0)$ is pinned at 2 (1). This explains both the pinning of $\langle n_1 \rangle + \langle n_2 \rangle$ and the jump in $\langle n_2 \rangle$ that are evident in Fig. 2(b).

Next we consider the case $U_2 = \Gamma_2$ representative of the crossover from a resonant dot 2 to an interacting one. Figure 3(a) plots $T\chi_{\text{imp}}$ vs T at different points along path O'A' in Fig. 1(b). Deep in the SC phase (e.g., $\varepsilon_1 = -U_1/125$) the system passes with decreasing temperature directly from a local-moment regime ($T\chi_{\text{imp}} = \frac{1}{4}$) to the SC limit ($T\chi_{\text{imp}} = 0$); just as for $U_2 = 0$, $\chi_{\text{imp}}(T = 0) = 0$. For ε_1 just above ε_1^+ [e.g., uppermost dashed line in Fig. 3(a)], $T\chi_{\text{imp}}$ instead evolves with decreasing T from near $\frac{1}{4}$ towards the value $\frac{1}{6}$ characterizing the $U_2 = 0$ QPT (a tendency seen more clearly [15] for $0 < U_2 \ll \Gamma_2$), then rises and reaches a plateau near $\frac{1}{4}$ before finally decreasing to zero. The manner in which $T\chi_{\text{imp}} \rightarrow 0$ as $T \rightarrow 0$ is identical to that in the Kondo regime of the conventional Anderson model [17], with $\chi_{\text{imp}}(T = 0) \simeq 0.1/T_K$ and T_K varying exponentially with $1/(\varepsilon_1 - \varepsilon_1^+)$ [inset to Fig. 3(b)]. For $\varepsilon_1 < \varepsilon_1^+$, $T\chi_{\text{imp}}$ approaches the FM value $\frac{1}{4}$ from above, but there is no temperature scale that vanishes on approach to the phase boundary. These behaviors are all indicative of the Kosterlitz-Thouless nature of the QPT, which holds for any $U_2 > 0$ (with the sole exception of the first-order QPTs that arise [8] only for two identical dots). Like the ferromagnetic Kondo model, whose properties it closely parallels, the small- U_2 FM phase exhibits singular Fermi liquid behavior with a quasiparticle density of states that diverges at the Fermi energy [12, 16].

The dot occupancies for $U_2 = \Gamma_2$ [Fig. 3(b)] show generally similar trends with ε_1 as for $U_2 = 0$ [Fig. 2(b)], but without jumps. Since p-h asymmetry is a marginal perturbation in the conventional Anderson model [17], $n_{\text{imp}}(T = 0)$ varies continuously with ε_1 , and there is no pinning of $\langle n_1 \rangle + \langle n_2 \rangle$ in either phase.

Comparison between Figs. 2 and 3 shows that for

$U_2 \lesssim \Gamma_2$, the properties retain their $U_2 = 0$ pseudogap character at high temperatures and/or far from the QPT. With decreasing U_2 (not shown), the pseudogap properties extend to lower values of T and $|\varepsilon_1 - \varepsilon_1^+|$.

Figure 4(a) shows the zero-temperature conductance vs ε_1 for $U_2 = \Gamma_2$ and four values of ε_2 . Deep in the FM phase (around $\varepsilon_i = -\frac{1}{2}U_i$), dot 1 is in Coulomb blockade and since there is no Kondo effect and hence no Kondo resonance, transport takes place solely through dot 2. For fixed ε_1 near $-0.25D = -\frac{1}{2}U_1$, g falls off as ε_2 is varied from $-\frac{1}{2}U_2$ (squares) to higher (circles and diamonds) or lower values, while for fixed ε_2 near $-\frac{1}{2}U_2$, the system passes through a QPT at $\varepsilon_1 = \varepsilon_1^+$, where g jumps. For ε_1 right above ε_1^+ or below ε_1^- , there is a Kondo effect centered primarily on dot 1, and due to interference between transport through the two dots, g is abruptly lowered. On moving deeper into the SC phase, the dot-1 occupancy moves further from 1, interference from transport through dot 1 is reduced, and g rises again. The preceding picture holds until dot 2 becomes sufficiently p-h asymmetric that the SC phase spans all values of ε_1 , and g vs ε_1 shows no sign of any QPT (triangles).

The conductance signatures of the QPT persist to $T > 0$, as illustrated in Fig. 4(b), which plots g vs ε_1 for $U_2 = \Gamma_2$ and $\varepsilon_2 = 0.075U_2$. Temperatures are expressed as multiples of $T_{K0} = 7 \times 10^{-4}D$, the Kondo scale when dot 2 is isolated ($\Gamma_2 = 0$) and dot 1 is at p-h symmetry ($\varepsilon_1 = -\frac{1}{2}U_1$). The foremost effect of increasing T is a progressive suppression of the Kondo effect, leading to a smoothing and weakening of the conductance dips in the vicinity of the QPTs, as well as shifts in the bottoms of the dips to larger $|\varepsilon_1 + \frac{1}{2}U_1|$.

Finally, we compare the regime $U_2 \lesssim \Gamma_2$ described above with the one $U_2 \gg \Gamma_2$ studied in previous works. The FM phase for small U_2 has an unquenched spin- $\frac{1}{2}$ residing predominantly on dot 1, which asymptotically decouples from the rest of the system, whereas for large U_2 a composite spin-1 formed by two dots is underscreened

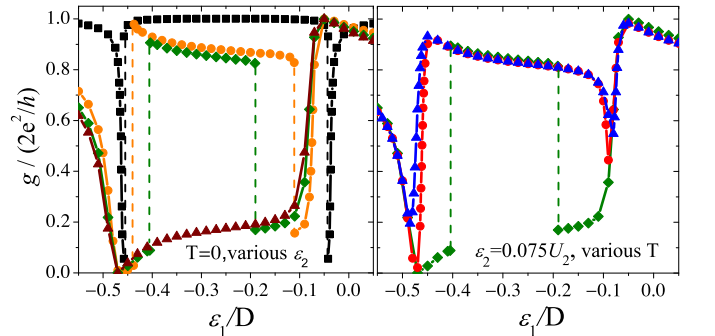


FIG. 4: (Color online). Linear conductance g vs ε_1 for $U_2 = \Gamma_2$. Left: Zero temperature and dot-2 level energies $\varepsilon_2/U_2 = -0.5$ (black \blacksquare), 0 (orange \bullet), 0.075 (green \blacklozenge), and 0.11 (brown \blacktriangle). Right: $\varepsilon_2 = 0.075U_2$ and temperatures $T/T_{K0} = 0$ (green \blacklozenge), 0.0057 (red \bullet), and 0.228 (blue \blacktriangle).

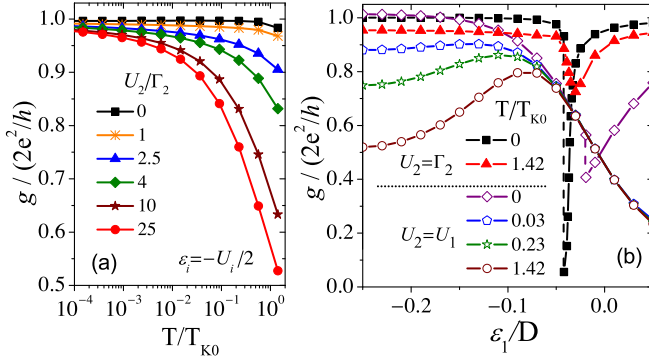


FIG. 5: (Color online). Conductance g plotted (a) vs T at p-h symmetry ($\varepsilon_i = -\frac{1}{2}U_i$); and (b) vs ε_1 for $\varepsilon_2 = -\frac{1}{2}U_2$, comparing the local-moment and underscreened spin-1 Kondo regimes of the FM phase, represented by $U_2 = \Gamma_2$ and $U_2 = U_1$, respectively.

by the leads to yield a strongly entangled spin- $\frac{1}{2}$ ground state [8, 9]. Since these two regimes belong to the same phase, they have similar singular Fermi-liquid properties as $T \rightarrow 0$ [16]. The question remains whether they may be distinguished through their behavior at higher T .

Figure 5(a) shows g vs T at the p-h-symmetric point $\varepsilon_i = -\frac{1}{2}U_i$ for six values of U_2 . For $U_2 \gg \Gamma_2$, the conductance drops significantly below its unitary limit once the temperature rises above the characteristic scale $T_K^{S=1}$ of the spin-1 Kondo effect, which is of order T_{K0} [8]. For $U_2 \lesssim \Gamma_2$, there is no Kondo physics in the FM phase and g remains close to $2e^2/h$ up to much higher temperatures of order Γ_2 . Figure 5(b) plots g vs ε_1 at different temperatures for $U_2 = -2\varepsilon_2 = \Gamma_2$ (path O'A' in Fig. 1) and for $U_2 = -2\varepsilon_2 = U_1$ (path O''A''). Just as in Fig. 5(a), the T dependence of the conductance in the FM phase is much weaker for $U_2 \lesssim \Gamma_2$ than for $U_2 \gg \Gamma_2$. Near p-h symmetry ($\varepsilon_1 = -0.25D$), the latter regime has $d^2g/d\varepsilon_1^2 > 0$ at all but the very lowest temperatures, reflecting the ε_1 dependence [8] of $T_K^{S=1}$, whereas $d^2g/d\varepsilon_1^2 \leq 0$ in the local-moment case. We conclude that the two regimes can be clearly differentiated via their conductance at temperatures (of order the typical Kondo scale T_{K0}) likely to be readily attainable in experiments.

In summary, we have studied two quantum dots coupled in parallel to metallic leads, focusing on situations where “dot 2” has a weaker on-site Coulomb interaction than “dot 1”: $U_2 < U_1$. For $U_2 \lesssim \Gamma_2$, the tunneling width of the dot-2 level, the properties still reflect the pseudo-gap Kondo physics found previously for $U_2 = 0$. For all $U_2 > 0$, Kondo-screened and free-moment phases are separated by quantum phase transitions of the Kosterlitz-Thouless type that have signatures in the electrical conductance up to experimentally accessible temperatures. In the free-moment phase, conductance measurements can also distinguish the small- U_2 regime, in which dot 1 carries a spin- $\frac{1}{2}$ and is essentially disconnected from the

rest of the system, from the regime $U_2 \gg \Gamma_2$ in which both dots contain strong electron correlations and their combined spin is partially screened by the leads. The two free-moment regimes have dot-lead entanglements that are markedly different from each other and from those in the Kondo phase. Given the feasibility of tuning between these three cases (and above an underlying zero-temperature phase transition) by adjusting just one gate voltage on each dot, this system offers fascinating possibilities from a quantum information perspective.

We thank D. Logan for helpful discussions. This work was supported by NSF DMR grants 0710540 and 0710581 in the US, and by CNPq and FAPESP in Brazil.

-
- [1] L. Kouwenhoven and L. Glazman, *Phys. World* **14**, 33 (2001).
 - [2] H. Jeong, A. M. Chang, and M. R. Melloch, *Science* **293**, 2221 (2001); J. C. Chen, A. M. Chang, and M. R. Melloch, *Phys. Rev. Lett.* **92**, 176801 (2004). N. J. Craig *et al.*, *Science* **304**, 565 (2004); A. Hübel *et al.*, *Phys. Rev. Lett.* **101**, 186804 (2008).
 - [3] R. M. Potok *et al.*, *Nature (London)*, **446**, 167 (2007).
 - [4] Y. Oreg and D. Goldhaber-Gordon, *Phys. Rev. Lett.* **90**, 136602 (2003); M. Pustilnik *et al.*, *Phys. Rev. B* **69**, 115316 (2004); M. R. Galpin, D. E. Logan, and H. R. Krishnamurthy, *Phys. Rev. Lett.* **94**, 186406 (2005).
 - [5] R. Žitko and J. Bonča, *Phys. Rev. B* **74**, 045312 (2006).
 - [6] L. G. G. V. Dias da Silva *et al.*, *Phys. Rev. Lett.* **97**, 096603 (2006).
 - [7] L. G. G. V. Dias da Silva, *et al.*, *Phys. Rev. B* **78**, 153304 (2008).
 - [8] D. E. Logan, C. J. Wright, and M. R. Galpin, *Phys. Rev. B* **80**, 125117 (2009).
 - [9] P. Nozières and A. Blandin, *J. Phys. (Paris)* **41**, 193 (1980); A. Posazhennikova and P. Coleman, *Phys. Rev. Lett.* **94**, 036802 (2005); P. Roura Bas and A. A. Aligia, *Phys. Rev. B* **80**, 035308 (2009).
 - [10] D. Withoff and E. Fradkin, *Phys. Rev. Lett.* **64**, 1835 (1990); R. Bulla, T. Pruschke, and A. C. Hewson, *J. Phys. Condens. Matter* **9**, 10 463 (1997).
 - [11] C. Gonzalez-Buxton and K. Ingersent, *Phys. Rev. B* **57**, 14 254 (1998).
 - [12] P. Mehta *et al.*, *Phys. Rev. B* **72**, 014430 (2005); W. Koller, A. Hewson, and D. Meyer, *ibid.* 045117 (2005).
 - [13] Y. Meir and N. S. Wingreen, *Phys. Rev. Lett.* **68**, 2512 (1992).
 - [14] R. Bulla, T. Costi, and T. Pruschke, *Rev. Mod. Phys.* **80**, 395 (2008).
 - [15] Preliminary results for the $U_2 > 0$ phase diagram, susceptibility, and zero-temperature conductance appeared in W. B. Lane, Ph.D. thesis, University of Florida, 2008.
 - [16] Analysis of the scattering phase shifts (to be reported elsewhere) indicates that the FM phase exhibits singular Fermi liquid behavior for all $U_2 > 0$.
 - [17] H. R. Krishna-murthy, J. W. Wilkins and K. G. Wilson, *Phys. Rev. B* **21**, 1003 (1980); *ibid.* 1044 (1980).